AD-A176 479 THE REPRESENTATION OF THE EARTH'S GRAVITATIONAL POTENTIAL IN A SPHERICAL (U) OHIO STATEUUNIV COLUMBUS DEPT OF GEODETIC SCIENCE AND SURVEYI... R H RAPP ET AL. 1/1

UNCLASSIFIED SEP 86 OSU/DGSS-372 AFGL-TR-86-0191 F/G 8/5 NL

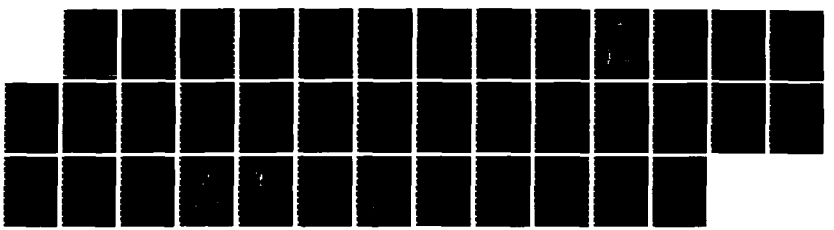

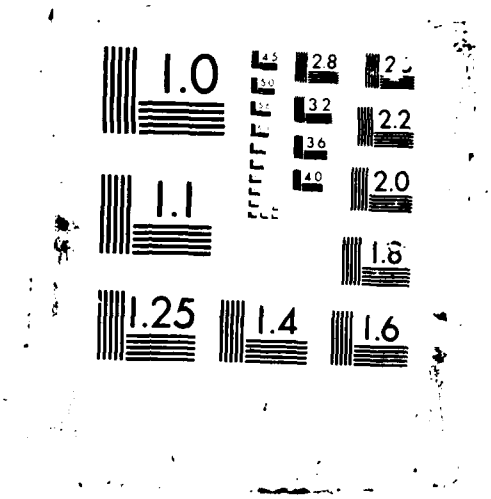
1.0
1.1
1.25
1.4
1.6
1.8
2.0
2.2
2.8
3.2
3.6
4.0

AFGL-TR-86-0191

THE REPRESENTATION OF THE EARTH'S GRAVITATIONAL POTENTIAL IN A SPHERICAL HARMONIC EXPANSION TO DEGREE 250

RICHARD H. RAPP
AND
JAIME Y. CRUZ

DEPARTMENT OF GEODETIC SCIENCE AND SURVEYING
THE OHIO STATE UNIVERSITY
COLUMBUS, OHIO 43210

SEPTEMBER 1986

SCIENTIFIC REPORT NO. 2

APPROVED FOR PUBLIC RELEASE; DISTRIBUTION UNLIMITED

AIR FORCE GEOPHYSICS LABORATORY
AIR FORCE SYSTEMS COMMAND
UNITED STATES AIR FORCE
HANSCOM AIR FORCE BASE, MASSACHUSETTS 01731

unclassified

SECURITY CLASSIFICATION OF THIS PAGE

AD-A194 6479

REPORT DOCUMENTATION PAGE

1a. REPORT SECURITY CLASSIFICATION Unclassified	1b. RESTRICTIVE MARKINGS
2a. SECURITY CLASSIFICATION AUTHORITY	3. DISTRIBUTION / AVAILABILITY OF REPORT Approved for public release; distribution unlimited
2b. DECLASSIFICATION / DOWNGRADING SCHEDULE	
4. PERFORMING ORGANIZATION REPORT NUMBER(S) OSU/DGSS Report No. 372	5. MONITORING ORGANIZATION REPORT NUMBER(S) AFGL-TR-86-0191
6a. NAME OF PERFORMING ORGANIZATION Department of Geodetic Science and Surveying 6b. OFFICE SYMBOL (If applicable)	7a. NAME OF MONITORING ORGANIZATION Air Force Geophysics Laboratory
6c. ADDRESS (City, State, and ZIP Code) The Ohio State University Columbus, Ohio 43210	7b. ADDRESS (City, State, and ZIP Code) Hanscom AFB Massachusetts 01731
8a. NAME OF FUNDING / SPONSORING ORGANIZATION 8b. OFFICE SYMBOL (If applicable)	9. PROCUREMENT INSTRUMENT IDENTIFICATION NUMBER F19628-86-K-0016
8c. ADDRESS (City, State, and ZIP Code)	10. SOURCE OF FUNDING NUMBERS PROGRAM ELEMENT NO. 62101F; PROJECT NO. 7600; TASK NO. 03; WORK UNIT ACCESSION NO AQ

11. TITLE (Include Security Classification)
The Representation of the Earth's Gravitational Potential in a Spherical Harmonic Expansion to Degree 250

12. PERSONAL AUTHOR(S)
Richard H. Rapp and Jaime Y. Cruz

13a. TYPE OF REPORT	13b. TIME COVERED	14. DATE OF REPORT (Year, Month, Day)	15. PAGE COUNT
Scientific No. 2	FROM _____ TO _____	1986 September	70

16. SUPPLEMENTARY NOTATION

17. COSATI CODES			18. SUBJECT TERMS (Continue on reverse if necessary and identify by block number)
FIELD	GROUP	SUB-GROUP	Geodesy; gravity; potential coefficients

19. ABSTRACT (Continue on reverse if necessary and identify by block number)

The gravitational potential of the earth has been represented in a spherical harmonic series that is complete to degree and order 250. This solution has been obtained by first carrying out a combination of satellite derived potential coefficients (GEML2') with a set of 1°x1° mean free air anomalies. These anomalies were formed from a merger of a June 1986 terrestrial set and a set derived from Geos-3/Seasat altimeter data. The combination solution was carried out after making downward continuation corrections to the surface anomalies and ellipsoidal corrections to the a priori potential coefficients. The adjustment yielded 582 potential coefficients and 64800 1°x1° anomalies. Two combination solutions were made, one (OSU86C) that excluded geophysically predicted anomalies and one (OSU86D) that included 5547 such anomalies. The potential coefficients ere determined through an optimal estimation procedure where, primarily, sampling error was minimized. Tests of the new solution were made by comparing undulation residuals at Doppler stations,

20. DISTRIBUTION / AVAILABILITY OF ABSTRACT	21. ABSTRACT SECURITY CLASSIFICATION
☐ UNCLASSIFIED/UNLIMITED ☐ SAME AS RPT ☐ DTIC USERS	unclassified
22a. NAME OF RESPONSIBLE INDIVIDUAL Christopher Jekeli	22b. TELEPHONE (Include Area Code) / 22c. OFFICE SYMBOL AFGL/LWG

DD FORM 1473, 84 MAR — 83 APR edition may be used until exhausted. All other editions are obsolete.

SECURITY CLASSIFICATION OF THIS PAGE
unclassified

1

Foreword

This report was prepared by Professor Richard H. Rapp, and Jaime Y. Cruz, Post-Doctoral Researcher, Department of Geodetic Science and Surveying, The Ohio State University, under Air Force Contract No. F19628-86-K-0016, OSU Project No. 718188. The contract covering this research is administered by the Air Force Geophysics Laboratory, Hanscom Air Force Base, Massachusetts, with Dr. Christopher Jekeli, Scientific Program Officer.

The computer resources provided at the Boeing Computer Center were provided by a grant from the National Science Foundation, EAR-8420862.

Computer resources at The Ohio State University were provided by contract funds and by the Instruction and Research Computer Center.

The orbit calculations were carried out at NASA's Goddard Space Flight Center with the cooperation and help of Mr. James Marsh and Mr. Steve Klc ɜko.

Mr. Vasilios Despotakis was most helpful in carrying out the estimation of the 1°x1° terrestrial mean anomaly field.

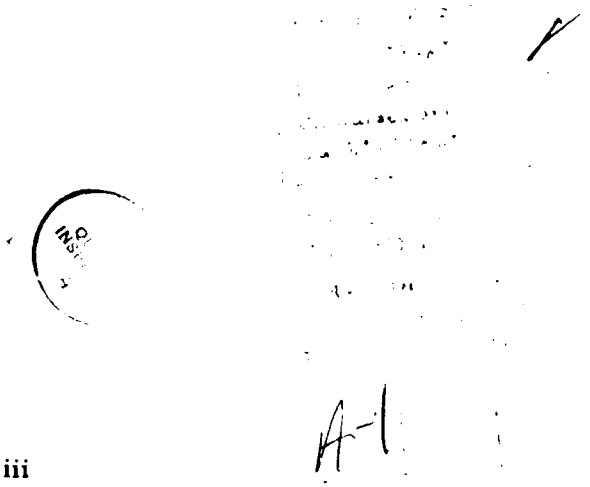

1. Introduction

The development of high degree spherical harmonic fields has been carried out for a number of years. The estimation of such fields has become more viable due to the availability of satellite altimeter data in the ocean areas, and the increased availability of terrestrial gravity measurements. One of the first solutions to degree 180 was that of Rapp (1978). In 1981 Rapp carried out a second expansion to degree 180 using a more complete set of a priori potential coefficients than used in the 1978 solution. Other solutions have been developed by Lerch et al (1981, GEM10C) and Wenzel (1985, GPM2).

In the past few years our studies have been related to improved modeling techniques taking into account approximations made earlier (Rapp,, 1984; Cruz, 1985) and in the improvement of our 1°x1° mean anomalies in land and ocean areas (Rapp, 1986a). The progress in these areas has led us to the development of new high degree expansions that take advantage of the new theory and new data. This report describes the data, methods, and analysis used in the development of the new solutions.

2. Data to be Used

We first describe each of the possible sources of data for use in the new solutions.

2.1 1°x1° Terrestrial Gravity Data

We have recently completed an update of our 1°x1° mean free air anomaly data set (Despotakis, 1986). This data set has evolved from prior compilations and from a merger with data made available from DMA Aerospace Center. The new data set contains 48,955 1°x1° anomalies (Figure 1) and 5689 anomalies estimated by geophysical correlation techniques. The location of most of the geophysical anomalies is shown in Figure 5. This new data set has corrected a number of errors found in the set used for the OSU81 solution and has incorporated a number of new data sources. The new data has led to better anomaly estimates for much of Europe, all of Australia, parts of Greenland, South Africa, India, Japan, Brazil, and other areas.

2.2 Altimeter Derived 1°x1° Gravity Anomalies

A combined Geos-3/Seasat altimeter data set has been used to derive gravity anomalies on a 0°.125 grid in the ocean areas. This gridded data has been used to obtain 30'x30' and 1°x1° mean free air anomalies (Rapp, 1986a). Approximately 37,000 values were estimated although some values were on land and some values were not reliable because of the sparsity of altimeter data in the area. The location of all anomalies is shown in Figure 2. In later use we will delete from this data set anomalies on land and values with large standard deviations.

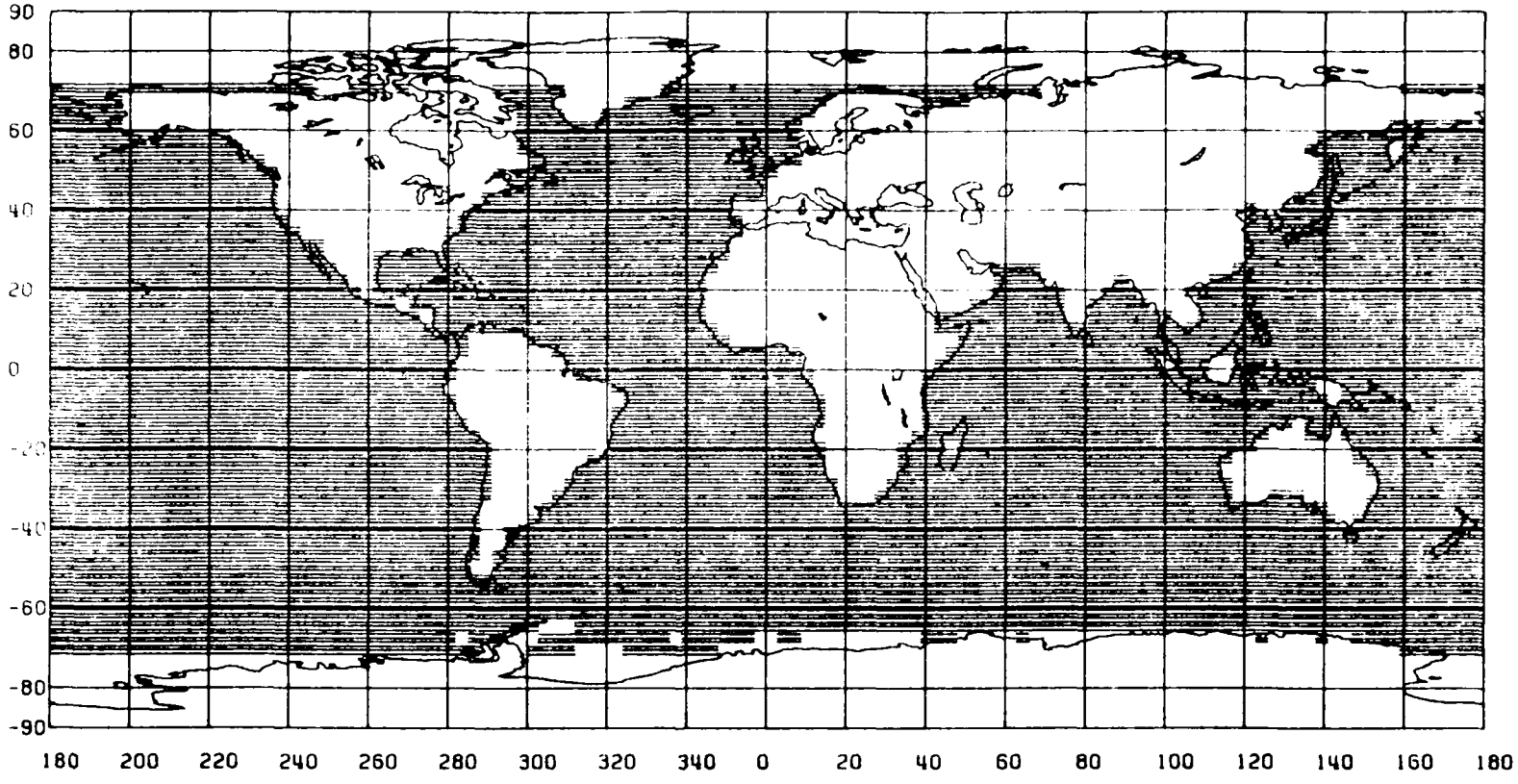

Figure 2. Location of 37,419 1°x1° Anomalies Derived From the Combined Geos-3/Seasat Altimeter Data

2. Use a terrestrial anomaly in ocean areas only if its standard deviation is $\leq$ 5 mgals or if no altimeter derived anomaly exists.

3. Do not use altimeter derived anomalies south of latitude -65°.

4. For accepted terrestrial data apply the following corrections:
   A. Due to Mass of Atmosphere (see equation (3.43))
   B. To Reduce Surface Anomaly to the Ellipsoid (see equation (3.30))
   C. For Gravity Formula Change

5. Reduce altimeter derived anomalies to the ellipsoid from the geoid using a gradient technique (see (3.30)).

6. Do not use altimeter derived anomalies in the Mediterranean area defined as ($30° \leq \phi \leq 50°$; $0° \leq \lambda \leq 40°$).

7. Create two data sets where one excludes geophysical anomalies and the other includes such anomalies. Preliminary tests indicated that 33 geophysical anomalies were very reasonable values and they were therefore included in the first data file. The location of these anomalies and the rational for their selection will be discussed later. We will be making two main combination solutions; one will be designated OSU86C and it will exclude geophysical anomalies (except for the select 33 values); the other will include the geophysical anomalies and will be designated OSU86D.

The location of the 50,562 1°x1° anomalies used for the OSU86C solution is shown in Figure 3 while Figure 4 shows the location of the 56,109 values used in the OSU86D solution. Figure 5 shows the location of 5,547 1°x1° anomalies used in OSU86D but not in OSU86C. Figure 6 shows the location of the 32,274 anomalies derived from the altimeter data that are used in both the C and D solutions.

In order to form a global field, values have to be estimated for blocks in which no anomaly estimate is available. Setting such values to zero is inconsistent with knowledge of the gravity field that we do have from the a priori potential coefficient estimates. We therefore calculated a rigorous anomaly on the ellipsoid using the potential coefficients described in Section 2.3.

The end product of this merger is two sets of 64,800 1°x1° anomalies that refer to an ellipsoid whose parameters were defined earlier and such that there is no atmosphere outside the ellipsoid. Each anomaly has been assigned a standard deviation which comes from the original estimation process. In the case of the anomaly "fill ins" we assigned a standard deviation of ±25 mgal. It is our intention to assume that all the anomaly estimates are independent. This is not the case and problems caused by our assumption will be discussed later.

We give in Table 1 information on the two 1°x1° anomaly fields to be used in our combination solution.

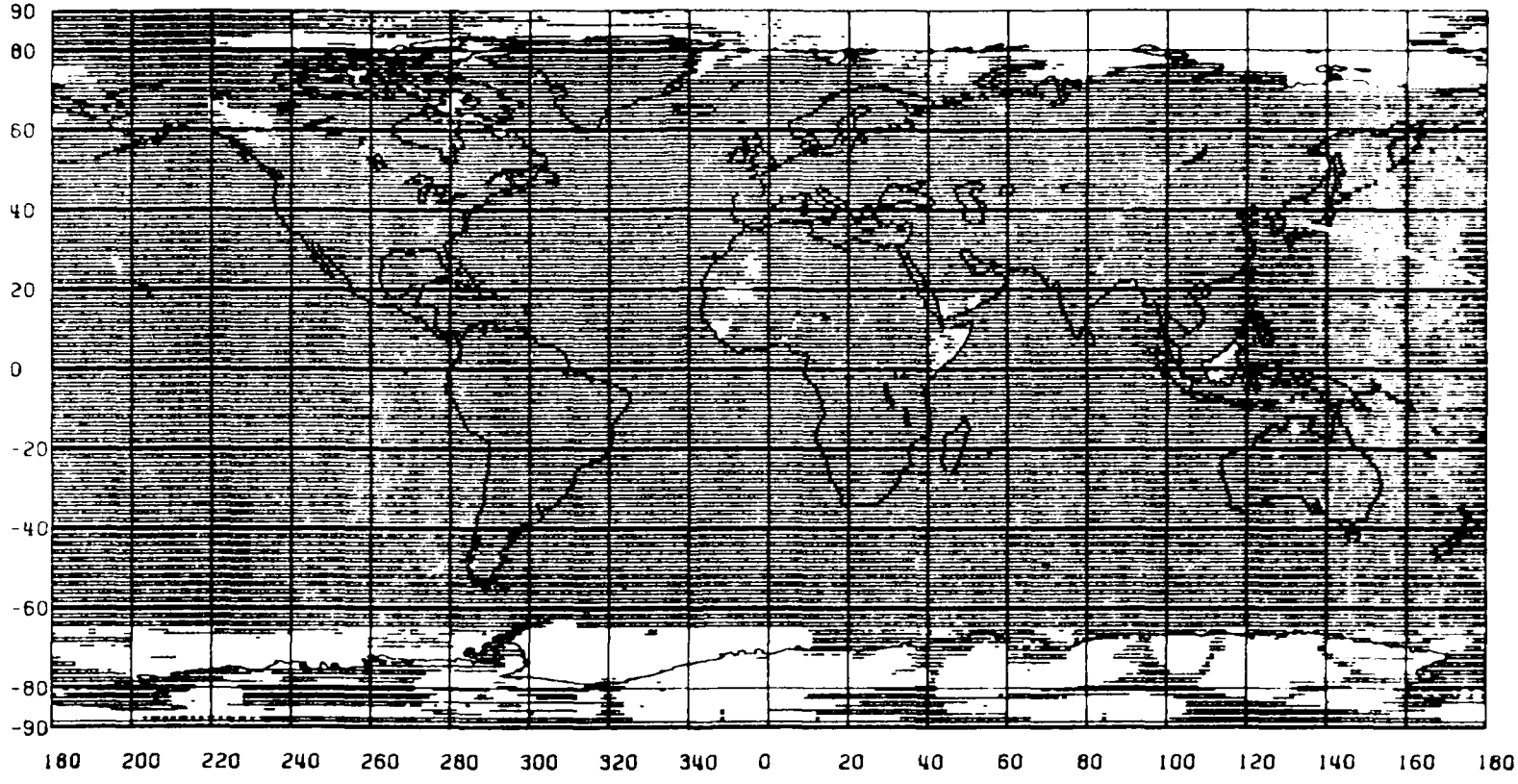

Figure 4. Location of 56,109 1°x1° Anomalies Used in OSU86D Solution Excluding Fill In Values

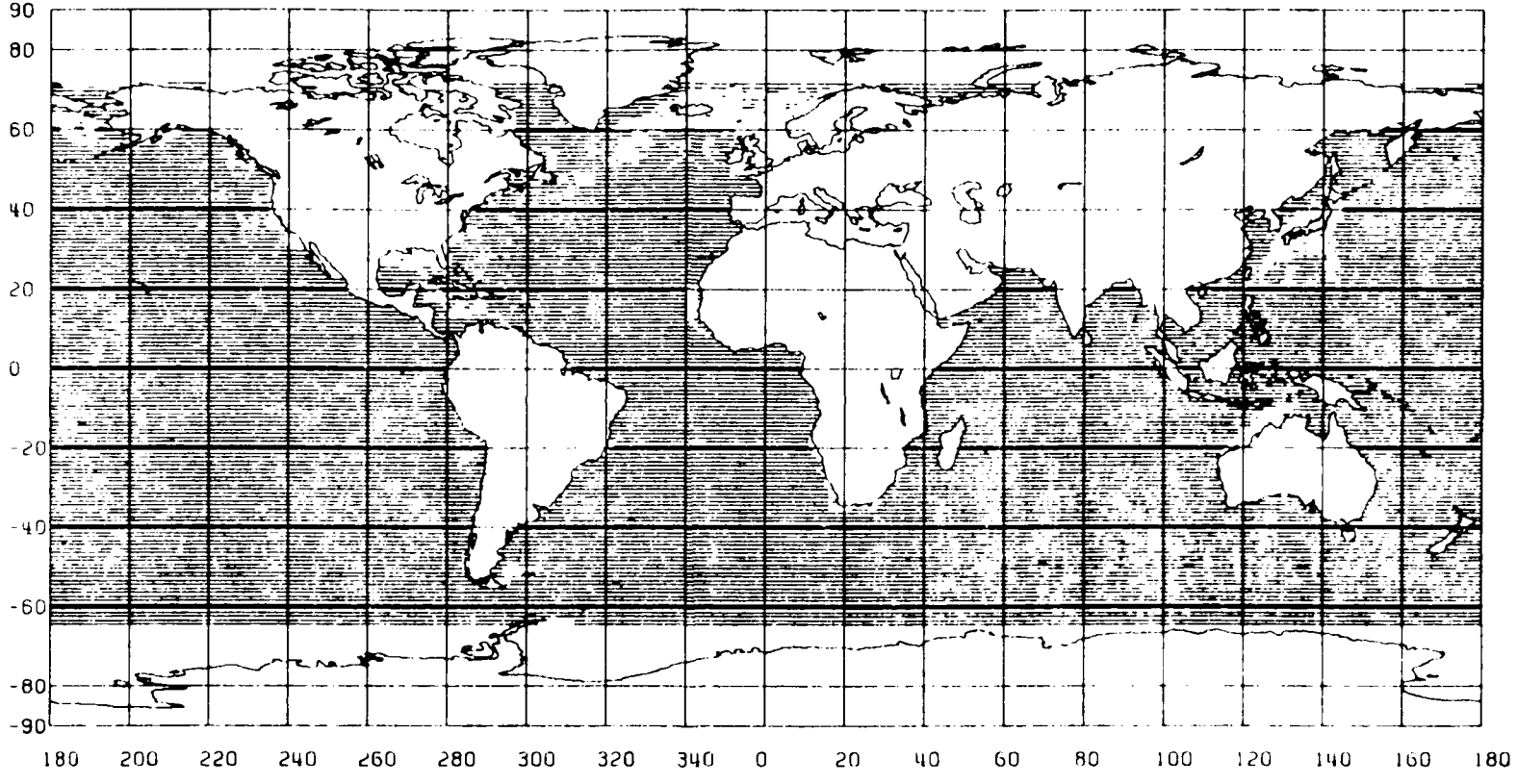

Figure 6. Location of 32,274 Altimeter Derived Anomalies in the Merged Data Set for Both the OSU86C and OSU86D Solutions

As normal figure of the earth a geocentric, rotating, equipotential ellipsoid, the gravity field of which can be defined by four parameters, is formally used. The parameters can be the equatorial radius a, the flattening f, the enclosed mass M which is equal to the earth's mass, and the rotational velocity ω which is equal to the earth's rotational speed. The normal gravity potential generated by this ellipsoid can be expressed in terms of even-degree zonal harmonics as:

$$U(r, \bar{\phi}, \lambda) = \frac{kM}{r}\left[1 + \sum_{n=2}^{\infty} \bar{D}_{2n,0}\bar{P}_{2n}(\sin\bar{\phi})\right] + \frac{1}{2}\omega^2 r^2 \cos^2\bar{\phi} \qquad (3.5)$$

where

$\bar{D}_{2n,0}$ fully normalized normal potential coefficients

$\bar{P}_{2n}$ fully normalized Legendre polynomials of degree 2n.

The $\bar{D}_{\ell,0}$ are related to the conventional J_ℓ coefficients as follows:

$$\bar{D}_{\ell,0} = \frac{-J_\ell}{\sqrt{2\ell + 1}} \qquad (3.6)$$

In practice the J_ℓ are negligible for $\ell > 6$. From Cook (1959) we can compute:

$$J_2 = \frac{2}{3}\left[f\left(1 - \frac{1}{2}f\right) - \frac{1}{2}m\left(1 - \frac{2}{7}f + \frac{11}{49}f^2\right)\right] \qquad (3.7)$$

$$J_4 = \frac{-4}{35}f\left(1 - \frac{1}{2}f\right)\left[7f\left(1 - \frac{1}{2}f\right) - 5m\left(1 - \frac{2}{7}f\right)\right] \qquad (3.8)$$

$$J_6 = \frac{4}{21}f^2(6f - 5m) \qquad (3.9)$$

with

$$m = \frac{\omega^2 a^3(1-f)}{kM} \qquad (3.10)$$

The disturbing potential is defined as:

$$T = W - U \qquad (3.11)$$

Using (3.2) and (3.5) this becomes:

$$T(r, \bar{\phi}, \lambda) = \frac{kM}{r}\sum_{\ell=2}^{\infty}\sum_{m=0}^{\ell}\sum_{\alpha=0}^{1}\left(\frac{a}{r}\right)^{\ell}\bar{C}_{\ell m}^{\alpha}\,\bar{Y}_{\ell m}^{\alpha}(\bar{\phi}, \lambda) \qquad (3.12)$$

where the fully normalized disturbing potential coefficients $\bar{C}_{\ell m}^{\alpha}$ are the same as the $\bar{A}_{\ell m}^{\alpha}$ except in the case of the even degree zonals for which the $\bar{D}_{\ell,0}$ are subtracted from the $\bar{A}_{\ell,0}$. In the usual notation:

$$\bar{C}_{\ell m}^{\alpha} = \left\{ \begin{array}{ll} \bar{C}_{\ell m}, & \alpha = 0 \\ \bar{S}_{\ell m}, & \alpha = 1 \end{array} \right\} \qquad (3.13)$$

$$\Delta g_M = -\left(\frac{1}{M} + \frac{1}{N} + \frac{2\omega^2}{\gamma} + \frac{e^4 r^3 \sin^2 2\bar{\phi}}{4b^4 M}\right) T - \frac{a^2}{N}\left(\frac{1}{r} + \frac{e^4 r^3 \sin^2 2\bar{\phi}}{4b^4}\right)\frac{\partial T}{\partial r} \qquad (3.17)$$

where

M meridional radius of curvature of the ellipsoid

N pr : vertical radius of curvature of the ellipsoid

b polar radius of the ellipsoid

Retaining only terms of $O(e^2)$ the boundary conditions (3.16) and (3.17) become (Cruz, 1986, (2.7), (3.10)):

$$\Delta g = -\frac{\partial T}{\partial r} - \frac{2}{r} T - e^2 \sin\bar{\phi}\cos\bar{\phi}\,\frac{\partial T}{r\partial\bar{\phi}} + e^2(3\sin^2\bar{\phi} - 2)\,\frac{T}{r} \qquad (3.18)$$

$$\Delta g_M = -\frac{\partial T}{\partial r} - \frac{2}{r} T + e^2(3\sin^2\bar{\phi} - 2)\,\frac{T}{r} \qquad (3.19)$$

If terms of $O(e^2)$ are further neglected the boundary condition transforms to the usual spherical form:

$$\Delta g^o = \Delta g_M^o = -\frac{\partial T}{\partial r} - \frac{2}{r} T \qquad (3.20)$$

where the superscript "o" denotes the spherical approximation gravity anomaly.

3.3 The Gravity Anomaly in Terms of Potential Coefficients

In our further discussions we concentrate on the use of the gravity anomaly Δg defined in (3.14) and the boundary condition (3.18), as opposed to the Δg_M of (3.15) and (3.19).

We first wish to express the gravity anomaly Δg of (3.14) in terms of the disturbing potential coefficients $\bar{C}_{\ell m}^{\alpha}$ occurring in (3.12). This is conceptually done by substituting (3.12) into (3.18). The result is formulated in Cruz (1986) in terms of ellipsoidal corrections:

$$\Delta g = \frac{kM}{r^2} \sum_{\ell=2}^{\infty} \sum_{m=0}^{\ell} \sum_{\alpha=0}^{1} (\ell-1)\left(\frac{a}{r}\right)^{\ell} (\bar{C}_{\ell m}^{\alpha} - \bar{C}_{\ell m}^{\alpha,h} - \bar{C}_{\ell m}^{\alpha,\gamma}) \bar{Y}_{\ell m}^{\alpha}(\bar{\phi}, \lambda) \qquad (3.21)$$

where the $\bar{C}_{\ell m}^{\alpha,i}$ ($i = h, \gamma$) are ellipsoidal corrections of $O(e^2)$ computed from the $\bar{C}_{\ell m}^{\alpha}$ themselves as follows:

$$\bar{C}_{\ell m}^{\alpha,i} = e^2(p_{\ell m}^i u_{\ell m} \bar{C}_{\ell-2,m}^{\alpha} + q_{\ell m}^i \bar{C}_{\ell m}^{\alpha} + r_{\ell m}^i v_{\ell m} \bar{C}_{\ell+2,m}^{\alpha}); \quad i = h, \gamma$$

with

$$\Delta g_a^0 = \frac{kM}{a^2} \sum_{\ell=2}^{\infty} \sum_{m=0}^{\ell} \sum_{\alpha=0}^{1} (\ell-1) \bar{C}_{\ell m}^{\alpha} \bar{Y}_{\ell m}^{\alpha}(\bar{\phi}, \lambda) \tag{3.28}$$

with inverse

$$\bar{C}_{\ell m}^{\alpha} = \frac{1}{\frac{kM}{a^2}(\ell-1)} \frac{1}{4\pi} \iint_{\sigma} \Delta g_a^0 \bar{Y}_{\ell m}^{\alpha}(\bar{\phi}, \lambda) \, d\sigma \tag{3.29}$$

We still need to relate the Δg_a^0 needed in (3.29) to the gravity anomaly that is more directly available in practice, namely, the gravity anomaly Δg_s that follows the definition (3.14) and refers to the topographic surface of the earth.

To relate Δg_s and Δg_a^0 Cruz (1985) has suggested that Δg_s be downward continued to the ellipsoid as a first step. To do this we utilize a Taylor series expansion:

$$\Delta g_E = \Delta g_s - \frac{\partial \Delta g}{\partial r} h - \frac{1}{2!} \frac{\partial^2 \Delta g}{\partial r^2} h^2 \ldots \tag{3.30}$$

where h is the height of the point (or mean elevation of a block) above the ellipsoid. In writing (3.30) we recognize the concern with analytical continuation and the problem of computing the gradient expressions. Although local gradients can be computed from detailed data, we need gradients for the reduction of mean anomalies on a global basis. The most efficient way to do this is to differentiate the anomaly expression (3.21) assuming potential coefficients are known. Neglecting the small effects of $C_{\ell m}^{\alpha,h}$ and $C_{\ell m}^{\alpha,\gamma}$ in these reductions we have:

$$\frac{\partial \Delta g}{\partial r} = - \frac{kM}{r^3} \sum_{\ell=2}^{\infty} \sum_{m=0}^{\ell} \sum_{\alpha=0}^{1} (\ell-1)(\ell+2) \left(\frac{a}{r}\right)^{\ell} \bar{C}_{\ell m}^{\alpha} \bar{Y}_{\ell m}^{\alpha}(\bar{\phi}, \lambda) \tag{3.31}$$

$$\frac{\partial^2 \Delta g}{\partial r^2} = \frac{kM}{r^4} \sum_{\ell=2}^{\infty} \sum_{m=0}^{\ell} \sum_{\alpha=0}^{1} (\ell-1)(\ell+2)(\ell+3) \left(\frac{a}{r}\right)^{\ell} \bar{C}_{\ell m}^{\alpha} \bar{Y}_{\ell m}^{\alpha}(\bar{\phi}, \lambda) \tag{3.32}$$

The root mean square value of the first derivative reduction in (3.30) is ±10 mgal (max = 19 mgals) and for the second derivative reduction it is ±0.01 mgal (max = 1.0 mgal) (Rapp, 1984). These computations were carried out with the Rapp (1981) potential coefficient field to degree 180. From recent calculations using 1°x1° mean gradient computation and an unpublished expansion to degree 300, the RMS value of the first derivative effect is ±0.8 mgal (max = 30 mgals) and for the second derivative it is ±0.04 mgal (max = 2.1 mgals). In practice we compute the gradient correction terms and store them for application to various sets of surface gravity anomalies.

Knowing the gravity anomaly Δg_E on the ellipsoid we can express the spherical approximation gravity anomaly Δg_a^0 on the equatorial sphere as (Cruz, 1986, (4.8)):

$$\Delta g_a^0 = \Delta g_E + \varepsilon_h + \varepsilon_\gamma + \varepsilon_1 + \varepsilon_2 + \varepsilon_3 + \ldots \tag{3.33}$$

and

$$\bar{C}_{\ell m}^{\alpha,2} = \frac{-e^4}{8(\ell-1)} [(\ell-5)(\ell-2)(\ell-1)K_{\ell-4,m}w_{\ell m}\bar{C}_{\ell-4,m}^{\alpha,0}$$
$$+ (\ell-3)(\ell)(\ell+1)L_{\ell-2,m}u_{\ell m}\bar{C}_{\ell-2,m}^{\alpha,0}$$
$$+ (\ell-1)(\ell+2)(\ell+3)M_{\ell m}\bar{C}_{\ell m}^{\alpha,0}$$
$$+ (\ell+1)(\ell+4)(\ell+5)N_{\ell+2,m}v_{\ell m}\bar{C}_{\ell+2,m}^{\alpha,0}$$
$$+ (\ell+3)(\ell+6)(\ell+7)P_{\ell+4,m}x_{\ell m}\bar{C}_{\ell+4,m}^{\alpha,0}] \qquad (3.39)$$

with

$$K_{\ell m} = \alpha_{\ell m}\alpha_{\ell+2,m}$$
$$L_{\ell m} = \alpha_{\ell m}(\beta_{\ell m} + \beta_{\ell+2,m})$$
$$M_{\ell m} = \alpha_{\ell m}\gamma_{\ell+2,m} + \beta_{\ell m}^2 + \alpha_{\ell-2,m}\gamma_{\ell m} \qquad (3.40)$$
$$N_{\ell m} = \gamma_{\ell m}(\beta_{\ell-2,m} + \beta_{\ell m})$$
$$P_{\ell m} = \gamma_{\ell-2,m}\gamma_{\ell m}$$

$$\alpha_{\ell m} = \frac{(\ell-m+1)(\ell-m+2)}{(2\ell+1)(2\ell+3)}$$
$$\beta_{\ell m} = \frac{(2\ell^2-2m^2+2\ell-1)}{(2\ell+3)(2\ell-1)} \qquad (3.41)$$
$$\gamma_{\ell m} = \frac{(\ell+m)(\ell+m-1)}{(2\ell+1)(2\ell-1)}$$

$$w_{\ell m} = \sqrt{\frac{(2\ell-7)(\ell+m-3)(\ell+m-2)(\ell+m+1)(\ell+m)}{(2\ell+1)(\ell-m-3)(\ell-m-2)(\ell-n-1)(\ell-m)}}$$
$$\qquad (3.42)$$
$$x_{\ell m} = \sqrt{\frac{(2\ell+9)(\ell-m+1)(\ell-m+2)(\ell-m+3)(\ell-m+4)}{(2\ell+1)(\ell+m+1)(\ell+m+2)(\ell+m+3)(\ell+m+4)}}$$

This completes the discussion on how to express the disturbing potential coefficients $C_{\ell m}^{\alpha}$ in terms of the surface gravity anomaly. The two steps involved are (3.30) followed by an implementation of (3.34) via (3.35) or (3.36). the formula for the $\bar{C}_{\ell m}^{\alpha,3}$ in terms of $\bar{C}_{\ell m}^{\alpha,0}$ is given in Cruz (1986, (6.20)).

3.5 Physical Realization of the Gravity Anomaly

A final point should be made concerning the physical realization of the theoretical gravity anomaly defined in (3.14). Rapp (1984) discusses the

The mathematical model is written as

$$F = F(L_\ell^a,\ L_x^a) = 0 \tag{4.1}$$

which is linearized to yield the observation equation:

$$B_\ell V_\ell + B_x V_x + W = 0 \tag{4.2}$$

where

$$B_\ell = \frac{\partial F}{\partial L_\ell};\qquad B_x = \frac{\partial F}{\partial L_x} \tag{4.3}$$

If we designate P_ℓ and P_x as the weight matrices for the observations and parameters respectively, the weighted least squares condition for the solution is:

$$V_\ell^T P_\ell V_\ell + V_x^T P_x V_x = \text{a minimum} \tag{4.4}$$

The solution for V_x is:

$$V_x = -(B_x^T M^{-1} B_x + P_x) B_x^T M^{-1} W \tag{4.5}$$

where

$$M = B_\ell P_\ell^{-1} B_\ell^T \tag{4.6}$$

The observation residuals are:

$$V_\ell = -P_\ell^{-1} B_\ell^T M^{-1} (B_x V_x + W) \tag{4.7}$$

The error variance-covariance matrix for the solution vector is:

$$\Sigma_x = m_o^2 (B_x^T M^{-1} B_x + P_x)^{-1} \tag{4.8}$$

where m_o^2 is the variance of unit weight.

The mathematical structure is formed by assuming that the potential coefficient estimate from satellite derived procedures should be the same as that obtained from the global gravity data set after appropriate corrections (e.g. ellipticity and downward continuations) have been made. We write:

$$F = L_x^a - L_{x_c}^a = 0 \tag{4.9}$$

If L_x^o is the approximate potential coefficient set and $L_x c^o$ is the coefficient set based on the observed (and corrected) anomalies, the misclosure vector is:

$$W = L_x^o - L_{x_0^c} \tag{4.10}$$

The $L_{x_0^c}$ values are computed from (see eq. 3.34)

$$\dot{C}_{\ell m}^{\alpha,o} - \frac{1}{4\pi\gamma(\ell-1)} \iint_\sigma \Delta g_E \dot{Y}_{\ell m}^\alpha(\phi,\ \lambda)\ d\sigma \tag{4.11}$$

The corresponding adjusted potential coefficients, considering the ellipsoidal corrections, would be:

$$\bar{C}_{\ell m,a} = L_{xa} + \delta\bar{C}_{\ell m}^{\alpha,o} + \bar{C}_{\ell m}^{\alpha,2} \qquad (4.21)$$

The adjusted anomalies would be found from:

$$L_{\ell a} = L_{\ell}^{o} + V_{\ell} \qquad (4.22)$$

The corresponding surface anomalies would be found from (4.13)

$$\Delta g_s = L_{\ell}^{a} - \delta g_A + \frac{\partial \Delta g}{\partial r} h + \frac{1}{2!} \frac{\partial^2 \Delta g}{\partial r^2} h^2 \qquad (4.23)$$

This completes the discussion of the adjustment model to be used in this combination solution. It is similar to the procedure used in the computation of the OSU78 combination solution except now we reduce surface anomalies to the ellipsoid and apply ellipsoidal corrections.

The normal equation matrix of the solution is given by $B_{\ell} P_{\ell}^{-1} B_{\ell}^{T}$. The size of the matrix is dependent on the number of a priori defined potential coefficients. For a solution complete to degree 20 the number of coefficients is 441. In the 1978 solutions we were able to complete a solution to $\ell = 12$. In our 1981 solution we wanted to go to a much higher degree with more coefficients. This could not be done because of computer limitations so we made certain assumptions that led to the normal equation matrix being diagonal. The result was an approximate combination solution that was carried out with small computer demands.

For the solution to be described in this report we have 64800 1°x1° "observations" and 582 unknowns. The estimated computer time for a solution on the IBM 4031D at OSU was 4.5 hours. As several solutions were contemplated the OSU computer requirements were still considered excessive. At this point we started tests on a CRAY XMP2/4 supercomputer at Boeing Computer Services. Funding for this computer work was from National Science Foundation Grant EAR-8420862. Modification of our existing combination program by one of us (JC) took advantage of the vectorization ability of the CRAY machine. With this change, a combination solution took 6.5 minutes. This meant that a number of different solutions could be carried out to learn what the best solutions could be.

5. The Estimation of the High Degree Potential Coefficients

The adjustment described in the previous section yields a set of adjusted potential coefficients (see eq 4.20) and a set of adjusted anomalies on the ellipsoid (see eq. 4.22). These anomalies can then be used to estimate $C_{\ell m}^{\alpha,o}$ using the following (see eq. 3.34)

$$\bar{C}_{\ell m}^{\alpha,o} = \frac{1}{\frac{kM}{a^2}(\ell-1)} \frac{1}{4\pi} \iint_{\sigma} \Delta g_{\ell} \bar{Y}_{\ell m}^{\alpha}(\phi, \lambda)\, d\sigma \qquad (5.1)$$

where $N = 180^\circ/\theta^\circ$. The evaluation of (5.2) using pre-computed associated Legendre function integrals, and a Fourier analysis of the mean anomalies along latitude bands, and with the q_ℓ values defined in (5.5) is carried out through the HARMIN subroutine in Colombo (ibid) as implemented in OSU (RHR) library program F419. This procedure is one of the ways in which the high degree expansions have been computed from the adjusted anomalies.

5.2 Potential Coefficients Through Optimal Estimation

A disadvantage of the procedure in the previous section is that it does not take into account data noise nor does it provide error estimates of the estimated coefficients. To consider this factors we have used the optimal estimation procedure developed by Colombo (1981) and implemented for 1°x1° data by Hajela (1984). We discuss only the general principles of this least squares collocation solution to (5.1). We start with the global mean gravity anomaly vector, $\underline{\Delta g}$, expressed as the sum of a signal vector, $\underline{z}$, and a noise vector, $\underline{n}$:

$$\underline{\Delta g} = \underline{z} + \underline{n} \tag{5.6}$$

Let the potential coefficient vector $[\bar{C}_{\ell m}^{\alpha,\circ}]$ be defined as $\underline{c}$. Let F be a linear operator that will estimate $\underline{c}$ (i.e. $\hat{\underline{c}}$) from $\underline{\Delta g}$:

$$\hat{\underline{c}} = \underline{F}(\underline{z} + \underline{n}) \tag{5.7}$$

The error in this estimation is $\underline{e}$:

$$\underline{e} = \underline{c} - \hat{\underline{c}} = \underline{c} - \underline{F}(\underline{z} + \underline{n}) = (\underline{c} - \underline{Fz}) - (\underline{Fn}) \tag{5.8}$$

We define the sampling error as $\underline{e}_s$ and the propagated noise error to be e_n. We have:

$$\underline{e}_s = \underline{c} - \underline{Fz} \; ; \quad \underline{e}_n = \underline{Fn} \tag{5.9}$$

The error covariance matrix of $\hat{\underline{e}}$ is:

$$E_T = E_s + E_n = M\{\underline{e}_s \, \underline{e}_s^T\} + M\{\underline{e}_n \, \underline{e}_n^T\} \tag{5.10}$$

where M is an averaging operator. Substituting (5.9) into (5.10) we find:

$$E_T = C - 2C_{cz}F^T + F(C_{zz} + D)F^T \tag{5.11}$$

where

$$C = M\{\underline{c} \, \underline{c}^T\}, \quad C_{cz} = M\{\underline{c} \, \underline{z}^T\}$$
$$C_{zz} = M\{\underline{z} \, \underline{z}^T\}, \; D = M\{\underline{n} \, \underline{n}^T\} \tag{5.12}$$

C represents the covariance matrix of the potential coefficients; C_{cz} is the cross covariance between the potential coefficients and the given mean

The error variance of the potential coefficients is the same for C^1 and C^2. It is given by:

$$\sigma^2_{c\ell m} = \sigma^2_{s\ell m} = \frac{1}{\gamma^2(\ell-1)^2}\left[\frac{c_\ell}{2\ell+1} - \begin{cases} \Delta\lambda^2 & \text{if } m = 0 \\ \dfrac{1-\cos m\Delta\lambda}{m^2} & \text{if } m \neq 0 \end{cases} - 2N \sum_{i=0}^{N-1} k^i_{\ell m}\, \chi^i_{\ell m}\right] \qquad (5.18)$$

where c_ℓ are the anomaly degree variances implied by an a priori potential coefficient model.

The calculation of the covariance functions and the potential coefficient errors of the optimum estimation solution requires the definition of c_ℓ. Adopted here was a model used by Colombo (ibid) which consists of the anomaly degree variances implied by the OSU78 solution from degree 2 to 100 and beyond 100 by a two component anomaly degree variance model described by Rapp (1979). Specifically this model (with the c_ℓ values interpreted to be at a sphere of radius R (= 6371 km) is:

$$c_\ell(R) = (\ell-1)\left[\frac{\alpha_1}{\ell+A}(s_1)^{\ell+2} + \frac{\alpha_2}{\ell+B}\frac{1}{\ell-2}(s_2)^{\ell+2}\right] \text{ mgals} \qquad (5.19)$$

where

$\alpha_1 = 3.4050, \quad \alpha_2 = 140.03$
$s_1 = 0.998006 \quad s_2 = 0.914232$
$A = 1, \quad B = 2$

For actual implementation we require the c_ℓ values on a sphere of radius a so we used:

$$c_\ell(a) = c_\ell(R)\left(\frac{R^2}{a^2}\right)^{\ell+2} \qquad (5.20)$$

A plot of this function will be given in a later section dealing with results.

Our intention in this study will be to implement both the HARMIN type solution and the optimal estimation solution. Various solutions will be made and the results compared.

6. Preliminary Investigations

Before we discuss our final solutions it is appropriate to describe a set of studies that led to the procedures used in the final solution. These studies were carried out with preliminary sets of global gravity models and a priori potential coefficient sets.

Table 3. Number of Anomaly Residuals as a Function of Residual Magnitude Range for Preliminary Combination Solutions

Range of Residual	Number of Residuals						
	nmax = 8 original m	nmax = 8 4 ≤ m ≤ 20	nmax = 8 5 ≤ m ≤ 15	nmax = 12 5 ≤ m ≤ 15	nmax = 12 8 ≤ m ≤ 15	nmax = 30 8 ≤ m ≤ 15	nmax = 30 12 ≤ m ≤ 15
0 - 2 mgal	50,553	50,568	50,587	51,298	50,713	49,427	47,682
2 - 4	8,055	8,745	10,685	10,713	12,322	13,198	14,693
4 - 6	3,369	3,999	2,524	1,672	1,071	1,312	1,812
6 - 8	1,820	795	793	612	435	520	376
8 - 10	465	428	195	360	187	165	135
10 - 12	290	227	12	121	65	92	63
12 - 14	151	24	1	22	7	52	34
14 - 16	75	8	3	1	0	31	5
16 - 18	8	2	0	0	0	3	0
18 - 20	6	3	0	1	0	0	0
20 → up	8	1	0	0	0	0	0

Merged data set: January 1983 Terrestrial Less Geophysical Anomalies + Altimeter Anomalies + Fill in Anomalies.

B. Cumulatively:

$$\delta N = \left[\sum_{\ell=2}^{N_{max}} \delta N_\ell^2 \right]^{1/2} \tag{6.2}$$

(2) The root mean square anomaly difference by degree and for the whole coefficient set:

A. By degree

$$\delta g_\ell = \left[\gamma^2 (\ell + 1)^2 \sum_{m=0}^{\ell} \sum_{\alpha=0}^{1} \Delta \bar{C}_{\ell m}^{2,\alpha} \right]^{1/2} \tag{6.3}$$

B. Cumulatively:

$$\delta g = \left[\sum_{\ell=2}^{N_{max}} \delta g_\ell^2 \right]^{1/2} \tag{6.4}$$

(3) The percentage difference by degree and cumulatively:

A. By degree:

$$P_\ell = \left[\frac{\sum_{m=0}^{\ell} \sum_{\alpha=0}^{1} \Delta \bar{C}_{\ell m}^{2,\alpha}}{\sum_{m=0}^{\ell} \sum_{\alpha=0}^{1} \bar{C}_{\ell m}^{2,\alpha}} \right]^{1/2} 100 \tag{6.5}$$

B. Average Percentage Difference

$$P = \frac{\sum_{\ell=2}^{N_{max}} P_\ell}{N_{max} - 1} \tag{6.6}$$

The values of δN and of δg represent the global mean difference of the two potential coefficient functions over the sphere. The values of δN_ℓ and δg_ℓ represent the same information by degree. The percentage difference provides information that takes into account the relative magnitude of the coefficient differences to the coefficient magnitudes.

Another quantity that can be used for the comparisons of two coefficient sets is the degree correlation coefficients (ρ_ℓ) and the overall correlation coefficient ρ. The degree correlation between the coefficient sets i and j would be:

$$\rho_\ell = \frac{\sum_{m=0}^{\ell} (\bar{C}_{\ell m_i} \bar{C}_{\ell m_j} + \bar{S}_{\ell m_i} \bar{S}_{\ell m_j})}{\left[\sum_{m=0}^{\ell} \sum_{\alpha=0}^{1} \bar{C}_{\ell m_i}^{2,\alpha} \right]^{1/2} \left[\sum_{m=0}^{\ell} \sum_{\alpha=0}^{1} \bar{C}_{\ell m_j}^{2,\alpha} \right]^{1/2}} \tag{6.7}$$

The overall correlation would be:

$$\rho = \frac{\sum_{\ell=2}^{N_{max}} \sum_{m=0}^{\ell} (\bar{C}_{\ell m_i} \bar{C}_{\ell m_j} + \bar{S}_{\ell m_i} \bar{S}_{\ell m_j})}{\left[\sum_{\ell=2}^{N_{max}} \sum_{m=0}^{\ell} \sum_{\alpha=0}^{1} \bar{C}_{\ell m_i}^{2,\alpha} \right]^{1/2} \left[\sum_{\ell=2}^{N_{max}} \sum_{m=0}^{\ell} \sum_{\alpha=0}^{1} \bar{C}_{\ell m_j}^{2,\alpha} \right]^{1/2}} \tag{6.8}$$

variances implied by a uniform uncorrelated error of ±10 mgals in 1°x1° blocks. From Rapp (1981), we have that the propagated standard deviation of a fully normalized potential coefficient of degree ℓ due to a uniform, uncorrelated error of m(Δg) in a block size of θ (radians) can be approximated as:

$$m(\bar{C},\ \bar{S}) = \frac{m(\Delta g)\theta}{2\gamma(\ell-1)\sqrt{\pi}} \qquad (6.9)$$

The 10 mgals used for m(Δg) in (6.9) is the root mean square (RMS) of the 8-15 mgal standard deviations used in the combination solution. The similarity between columns (3) and (5) is evident.

To examine whether the assumption of 8-15 mgal uncorrelated errors was reasonable we computed a set of potential coefficients from only the unadjusted 1°x1° anomalies. These values were then differenced from the unadjusted GEML2′ coefficients. The difference anomaly degree variances were then computed and shown in Table 5, column (2). It is seen that the data errors shown in columns (1) and (3) cannot account for the differences shown in column (2). This implies that the 8-15 mgal uncorrelated noise assumption is very optimistic.

We decided to examine the use of an RMS standard deviation of ±25 mgals for the 1°x1° anomalies. The assumption of uniform uncorrelated errors leads to error anomaly degree variances that are shown in Table 5, column (4). These variances are now $(25/10)^2 = 6.25$ times larger than those of the ±10 mgal accuracy, and appear to be much more reasonable. The ±25 mgal RMS accuracy could be implemented in our combination solution by multiplying the 8-15 mgal accuracies by 2.5 then restricting the range to $20 \leq m \leq 38$ mgals. We then performed a combination solution denoted by CS(20, 38), yielding error anomaly degree variances for the adjusted coefficients as shown in Table 5, column (6). These values are now larger, with cumulative variance to degree 20 of 1.88 mgal^2 compared with 0.48 mgal^2 from column (5).

It is of interest to compare the coefficients of the CS(8, 15) and CS(20, 38) solutions in terms of undulation and anomaly differences and percentage differences. Using the equations of section 6.2 the difference between the two solutions are shown in Table 6. As would be expected the greatest change takes place at the lower degrees because it is here that the dual estimate of the potential coefficients are obtained from the adjustment of satellite and terrestrial data.

The CS(8, 15) and CS(20, 38) types of solution were also compared in terms of orbit fits and fits to Doppler derived undulations. The orbit fit results are shown in Table 7, with more specific details of orbit tests given in Section 8.5. It is seen that the CS(20, 38) solution performs substantially better than the CS(8, 15). This seems natural as the higher anomaly standard deviations gives the a priori potential coefficients greater influence on the solution.

Table 8. Comparison of Doppler Derived Undulations with Preliminary Geopotential Models Complete to Degree 180.

Model	Mean Difference	Std Dev. Difference	Number of Stations	Area
CS(8,15)	0.32 m	±1.64 m	1749	Global[1]
CS(20,38)	0.19	1.68	1738	
CS(8, 15)	0.38	1.55	691	N. America[1]
CS(20, 38)	0.21	1.54	687	
CS(8,15)	-0.24	1.42	172	Europe[2]
CS(20, 38)	-0.48	1.38	172	
CS(8, 15)[3]	-1.13	1.60	114	Australia[2]
CS(20, 38)	-1.06	1.69	114	

[1] stations with residuals greater than 4 meters in absolute value were rejected

[2] A fixed set of stations was used

[3] The combination solution used an anomaly standard deviation range of $8 \leq m \leq 15$ mgals over the land of Australia only, with $20 \leq m \leq 38$ mgals used over the rest of the world.

difference standard deviation of ±1.60 m at 114 Australian Doppler stations with our final solution to be discussed later, compared with ±1.69 when the CS(20, 38) solution was used.

The problems discussed in this section arise from the assumption of uncorrelated noise. In fact the anomaly errors are correlated. Such correlation and its role in the computation of anomaly degree variance accuracies is discussed by Weber and Wenzel (1982). At this point we have no way of treating anomaly error correlation in our solutions. Instead we have increased our anomaly error estimates. Such a procedure is not desirable and in fact gives unreasonably high errors at degrees above 30. To compensate for this, our accuracy estimate for unadjusted coefficients will be based on the ±10 mgal uncorrelated noise assumption.

6.4 Preliminary High Degree Expansions

We next studied the manner by which the high degree expansions from the adjusted anomalies of the combination solution should be carried out. The main comparisons to be discussed here relate to a HARMIN type solution (see equation 5.2) and the optimal estimation solution (see equation 5.15). The first

implied by the OE(8, 15) and OE1 test solutions as well as the a priori model used in the optimal estimation procedure. The smoothing effect of the anomaly noise is evident from this plot.

The optimal estimation procedure yielded error estimates for the computed coefficients. For the OE(8, 15) solution these estimates were directly taken, giving error anomaly degree variances as also plotted in Figure 7. For the OE1 solution the error estimates from the optimal estimation mainly correspond only to the sampling error, with a small contribution from the 1 mgal noise. To complete these estimates we quadratically added the propagated error implied by the assumption of ±10 mgal uniform, uncorrelated 1°x1° noise. Specifically, we computed:

$$m(\bar{C}, \bar{S}) = \sqrt{m^2(SE) + m^2(PE)} \qquad (6.11)$$

where m(SE) is the sampling error and m(PE) is the propagated error. The m(PE) is given by (6.9). A similar, but not as rigorous procedure was used in the development of the OSU81 field. The total error estimate for the OE1 solution gave error anomaly degree variances that are also shown in Figure 7.

The error estimates for the OE(8, 15) solution are smaller than the total error estimates of the OE1 solution. This is consistent with the concept of filtering the anomaly errors in the OE(8, 15) solution. However, this filtering involved a smoothing of the spectrum which could substantially affect valid information. In order to test the two solutions we compared then in terms of their fits to Doppler derived undulations as shown in Table 10. The OE1 solution performed slightly better in these comparisons. At this point we decided to use for our work the OE1 type of solution, with a simple propagation of the anomaly errors as shown in (6.11).

Since the optimal estimation solution is a complicated process it is of interest to compare the results of HARMIN with OE1. These comparisons are shown in Table 11. The conclusion from Table 11 is that HARMIN gives coefficients that agree well with the coefficients found from the optimal estimation. The disadvantage of the HARMIN solution is that no error estimates are provided. Such values are found when the optimal solution is carried out.

Table 10. Comparison of OE(8, 15) and OE1 in Terms of Fits to Doppler Derived Undulations. Maximum Degree is 180.

Model	Mean Difference	Std Dev. Difference	Number of Stationst	Area
OE(8,15)	0.22 m	±1.68 m	1731	Global
OE1	0.19	1.68	1738	
OE(8, 15)	0.25	1.56	683	N. America
OE1	0.21	1.54	687	

† Stations with residuals greater than 4 meters in absolute value were rejected

Table 11. Comparison of Potential Coefficient Solutions From HARMIN and from Optimal Estimation (1 mgal standard error).

ℓ	δN (cm)	δg (mgals)	P(%)
2	0.0	0.00	0.0
10	0.0	0.00	0.0
20	0.0	0.00	0.0
30	0.2	0.01	0.5
50	0.2	0.02	1.1
75	0.8	0.09	6.2
100	1.0	0.15	10.6
120	1.0	0.18	13.2
150	0.6	0.14	13.0
180	0.8	0.22	22.3
to 180	8.9	1.53	7.6

6.5 A Study of the Undulation Residual Correlation with Elevation

Tscherning (1985, private communication) pointed out that the differences in the Doppler and gravity model undulations were correlated with elevation for the OSU81 solution but not for the GPM2 field. In our research we have computed this correlation for several models for various Doppler data sets by assuming there was a linear correlation with elevation. To do this the available Doppler stations were grouped into 100-meter elevation intervals. The undulation residuals ΔN falling within an interval were then averaged to get ΔN. The mean value ΔN was assumed to refer to the mean elevation H of the stations involved. A simple least squares fit was then carried out to compute the slope s and bias b in the observation equation:

Table 12. Undulation Residual Correlation with Elevation Using the Global Station Set. Maximum Degree is 180.

Solution	Slope (m/km)	Std. Dev. (m/km)	Number of Stations†
OSU81	0.73	±0.16	1721
GPM2	0.00	0.10	1735
CS(20, 38, OE1)	0.39	0.13	1738
GPM2(n = 7 to 14) + CS(20, 38, OE1)	0.02	0.13	1734
CS(8, 15, OE1)	0.42	0.13	1749

† stations with residuals greater than 4 meters in absolute value were rejected

The slopes of our new solutions are less than in OSU81 (~0.4 m/km compared to ~0.7 m/km), although they may still be considered significant. Further tests are needed to better understand the apparent slope problem and its implications.

Table 13. Undulation Residual Correlation with Elevation Using the Global Station Set. Maximum Degree is 30.

Solution	Slope (m/km)	Std. Dev. (m/km)	Number of Stations†
OSU81	0.93	±0.18	1694
GPM2	0.24	0.17	1725
GEML2	0.57	0.21	1619
GRIM3L1	0.79	0.19	1693
CS(20, 38, OE1)	0.74	0.17	1731

† Stations with residuals greater than 5 meters in absolute value were rejected.

In addition we found, again through Doppler undulation comparisons, some geophysical anomalies to be quite realistic in the sense that they yield improved undulation values at selected sites. Because of this we selected (see Section 6.6) 33 geophysical anomalies to be included in the data set for which almost all geophysical anomalies were excluded. The formation of this global data set was discussed in Section 2.4.

Tests with these fields indicated that our Doppler undulation comparisons in Australia were not as good as found in other areas, primarily North America and Europe. In order to obtain a better Doppler fit in the Australia region we gave the terrestrial anomaly data higher weight by specifying in this region the anomaly standard deviation range to be 8 to 15 mgals instead of the 20 to 38 mgal used everywhere else (see Section 6.3). In addition we changed five anomalies from one data source to another source on the basis of individual Doppler undulation comparisons. This led to undulation differences decreasing from ±1.69 m to ±1.60 m. More details of undulation comparisons are given in Section 8.

With the above as background we carried out the two main solutions of this report, OSU86C and OSU86D. The C solution essentially excludes geophysical anomalies while the D solution includes them. The combination solutions were performed on a CRAY XMP 2/4 machine using the procedures outlined in our previous sections. The ellipsoidal corrections were applied to the adjusted coefficients (see eq. 4.21) to obtain our final "adjusted" coefficients. The adjusted anomalies were developed into potential coefficients using the optimal estimation procedure with a uniform anomaly noise of ±1 mgal and the a priori anomaly degree variance model defined by equations 5.19 and 5.20. The expansion was carried out to degree 250 which involves the determination of 63,001 coefficients. The coefficients were merged with the adjusted coefficients (see remark below eq. 5.1), ellipsoidal corrections computed from the merger (eqs. 3.37 and 3.39), and these corrections applied (eq. 3.36) to obtain the final high degree coefficient set. Although the adjusted coefficients and the coefficients computed from the adjusted anomalies should be the same, we gave preference to the directly adjusted potential coefficients because such coefficients carried a standard deviation determined through the adjustment.

The standard deviations for the potential coefficients not estimated in the adjustment were obtained considering the sampling error (SE), found from the optimal estimation solution (see eq. 5.18) and a propagated error (PE) implied by the assumption of ±10 mgal uncorrelated noise for the 1°x1° anomalies. This error is computed from:

$$m(PE) = \frac{m(\Delta g)\theta}{2\gamma(\ell + 1)\sqrt{\pi}} \qquad (7.1)$$

where θ is the block size (1° in radians) and $m(\Delta g)$ is the anomaly standard deviation in units of γ. The coefficient error, for either C or S was then:

$$m(C, S) = \sqrt{m^2(SE) + m^2(PE)} \qquad (7.2)$$

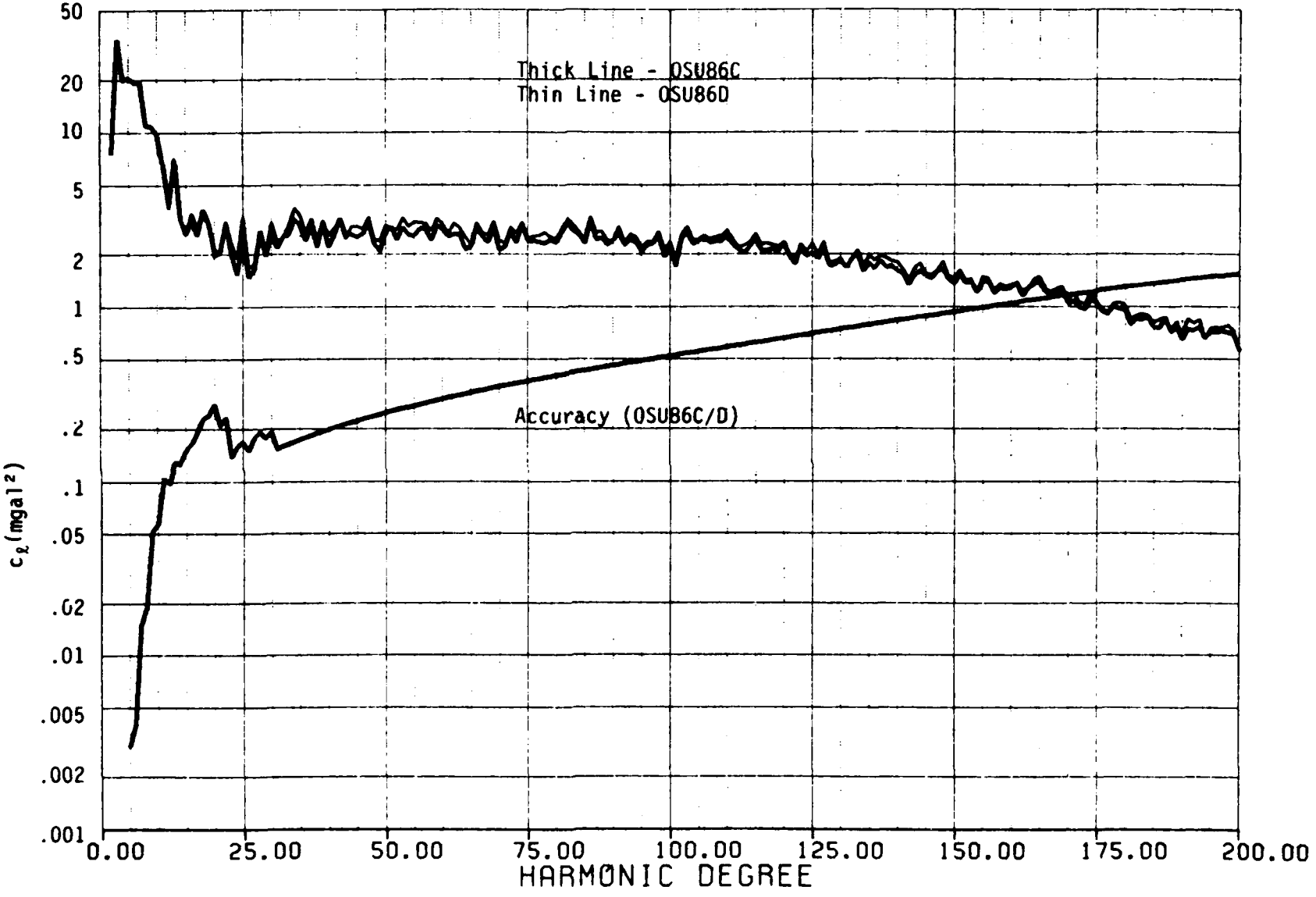

Figure 8. Anomaly Degree Variances and Their Accuracy for OSU86C and OSU86D

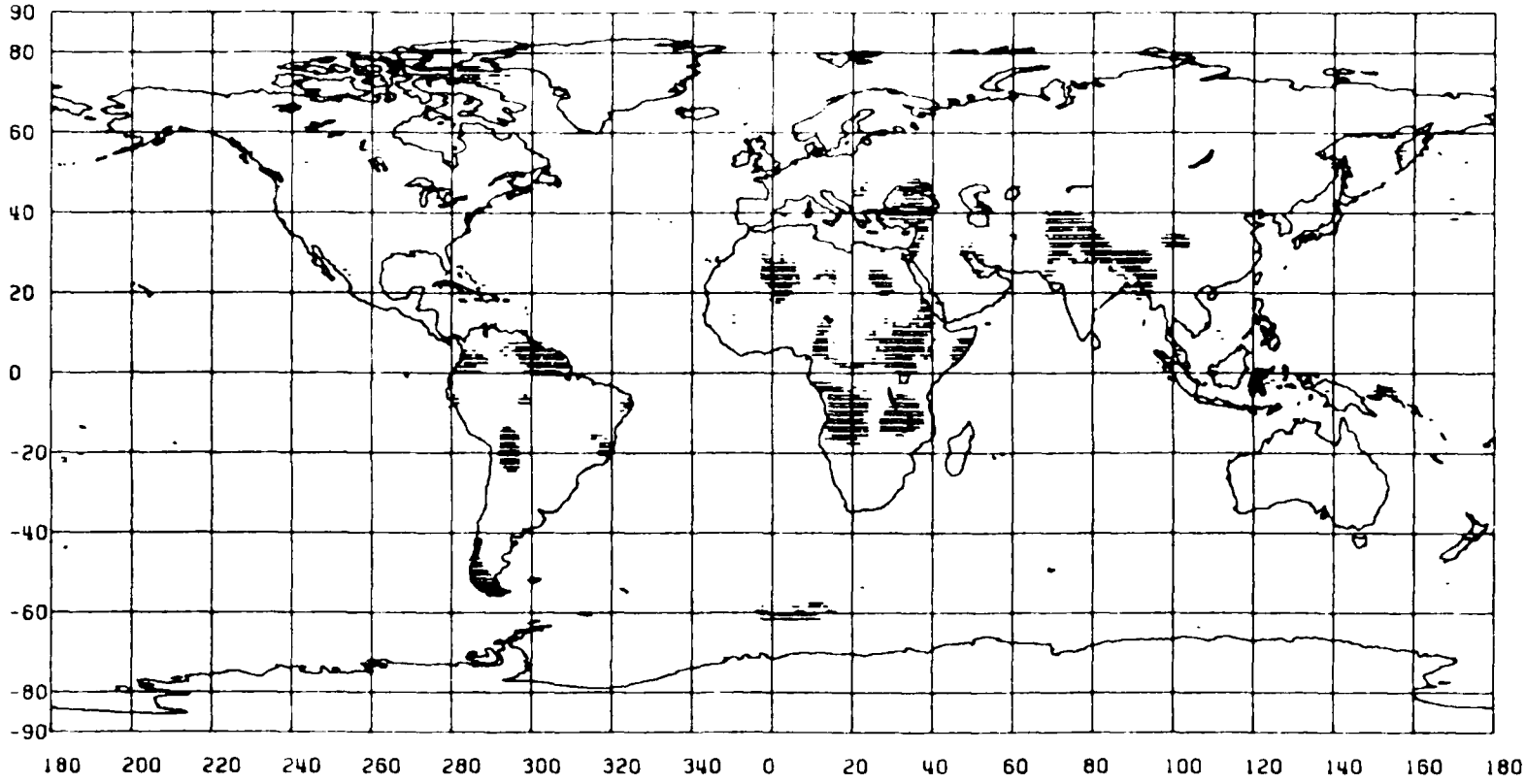

Figure 10. Location of 1,476 Residuals That Exceeded 7 mgals in the OSU86C Solution

8. Comparison of Results

The purpose of this section is to compare the new models between themselves and with two other high degree models. The models are the OSU81 (Rapp, 1981) and the GPM2 (Wenzel, 1985) model. The comparisons, carried out in several different ways are described in the following section.

8.1 Anomaly and Undulation Comparison

The global differences between the various solutions are shown in Table 15 for undulations and Table 16 for anomalies. The differences are given for the maximum degrees of 30 and 180.

Table 15. Potential Coefficient Differences in Terms of Geoid Undulations (meters)

	OSU86D	OSU86C	GPM2
OSU Dec81			
to ℓ = 30	± 1.04	± 1.32	± 1.12
to ℓ = 180	1.20	1.51	1.31
GPM2			
to ℓ = 30	± 1.08	1.21	
to ℓ = 180	1.25	1.43	
OSU86C			
to ℓ = 30	± 0.56		
to ℓ = 180	0.73		

Table 16. Potential Coefficient Differences in Terms of Gravity Anomalies (mgals)

	OSU86D	OSU86C	GPM2
OSU Dec81			
to ℓ = 30	± 2.5	± 3.0	± 2.6
to ℓ = 180	7.3	8.9	8.4
GPM2			
to ℓ = 30	± 2.6	3.0	
to ℓ = 180	8.5	9.9	
OSU86C			
to ℓ = 30	± 1.5		
to ℓ = 180	4.9		

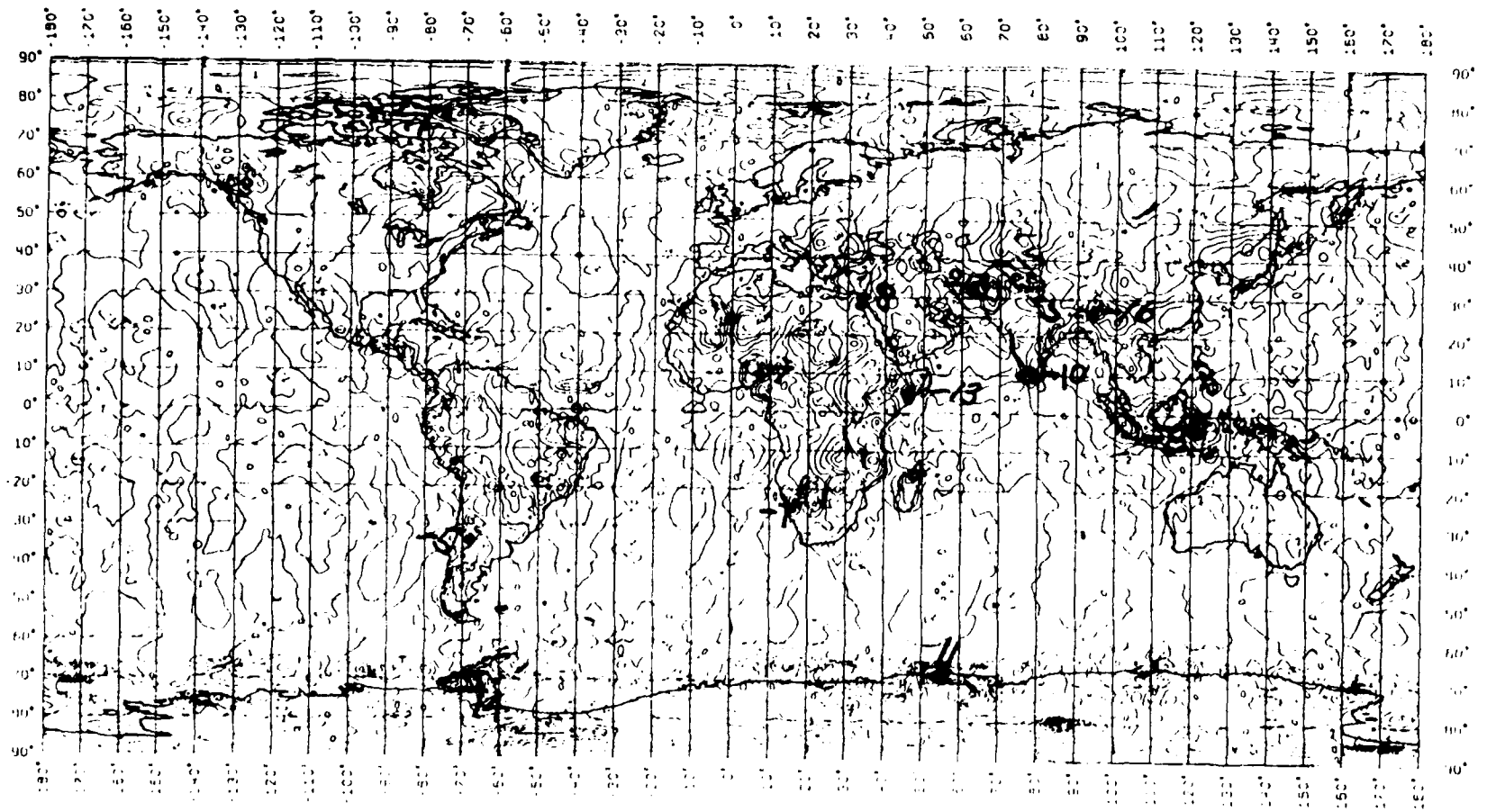

Figure 12. Geoid Undulation Difference Map - OSU86D Minus GPM2 (Contour Interval is 1 m based on a 2° x 2° grid)

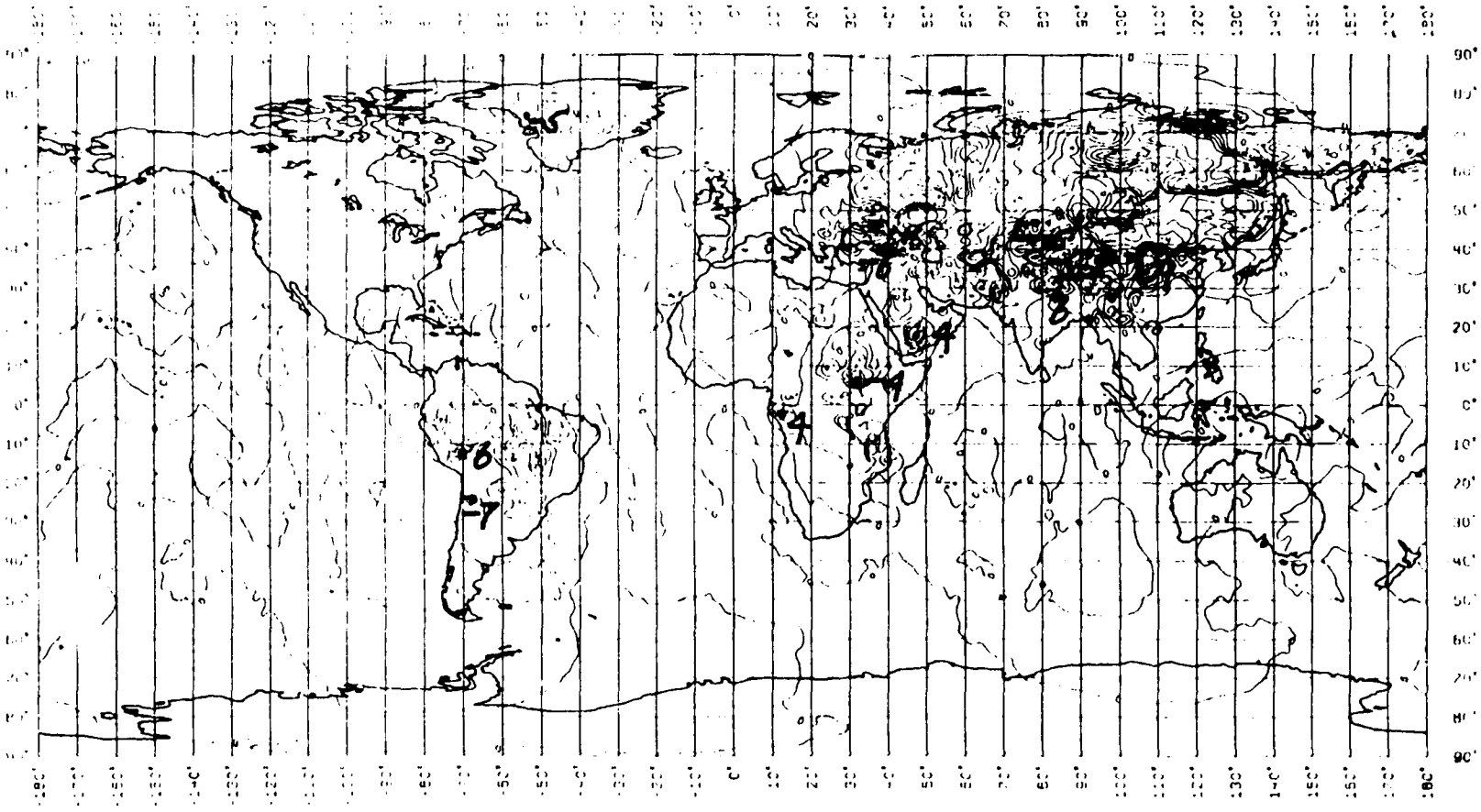

Figure 14. Geoid Undulation Difference Map OSU86C Minus OSU86D (Contour Interval is 1 m based on a 2° x 2° grid)

8.3 Doppler Undulation Comparisons

We next turn to a comparison of the geoid undulations derived from the various geopotential models with undulations derived from Doppler derived positions. If h is the ellipsoidal height of a station derived through Doppler satellite positioning techniques, after conversion to a geocentric system properly scaled (Rapp, 1983), the "Doppler undulation" is:

$$N_o - h_o - H \qquad (8.1)$$

where H is the orthometric height of the point. We compute N from Brun's equation where the disturbing potential is given by equation (3.12) with r the geocentric distance to the point in question projected to the ellipsoid. In all our comparisons we used the parameters to convert the Doppler system to a geocentric system with correct scale derived by Boucher and Altamimi (1985). The translation and scale parameters to go from the Doppler system to a geocentric system were used as follows:

$\Delta x = -10.6$ cm

$\Delta y = 69.7$ cm

$\Delta z = 490.1$ cm

$\Delta s = -0.604$ ppm

The comparisons made were with two primary sets of Doppler stations. One contained approximately 800 stations and was received from Tscherning. This set was originally obtained from the National Geodetic Survey and contains stations only in North America. The second set contained approximately 2000 stations distributed globally. The coordinates were determined in the years from 1971 to 1985. The number of passes could range from a minimum of 25 to a maximum of 592. In our analysis we made no correction for sun spot effects as suggested by Tscherning and Goad (1985). The overall effect of neglecting this for our large data sets is expected to be only a few cm. In making our comparison we assumed the geoid undulations referred to an ellipsoid with equatorial radius of 6378136 m and a flattening of 1/298.257. Comparisons for the Tscherning data set are given in Table 19.

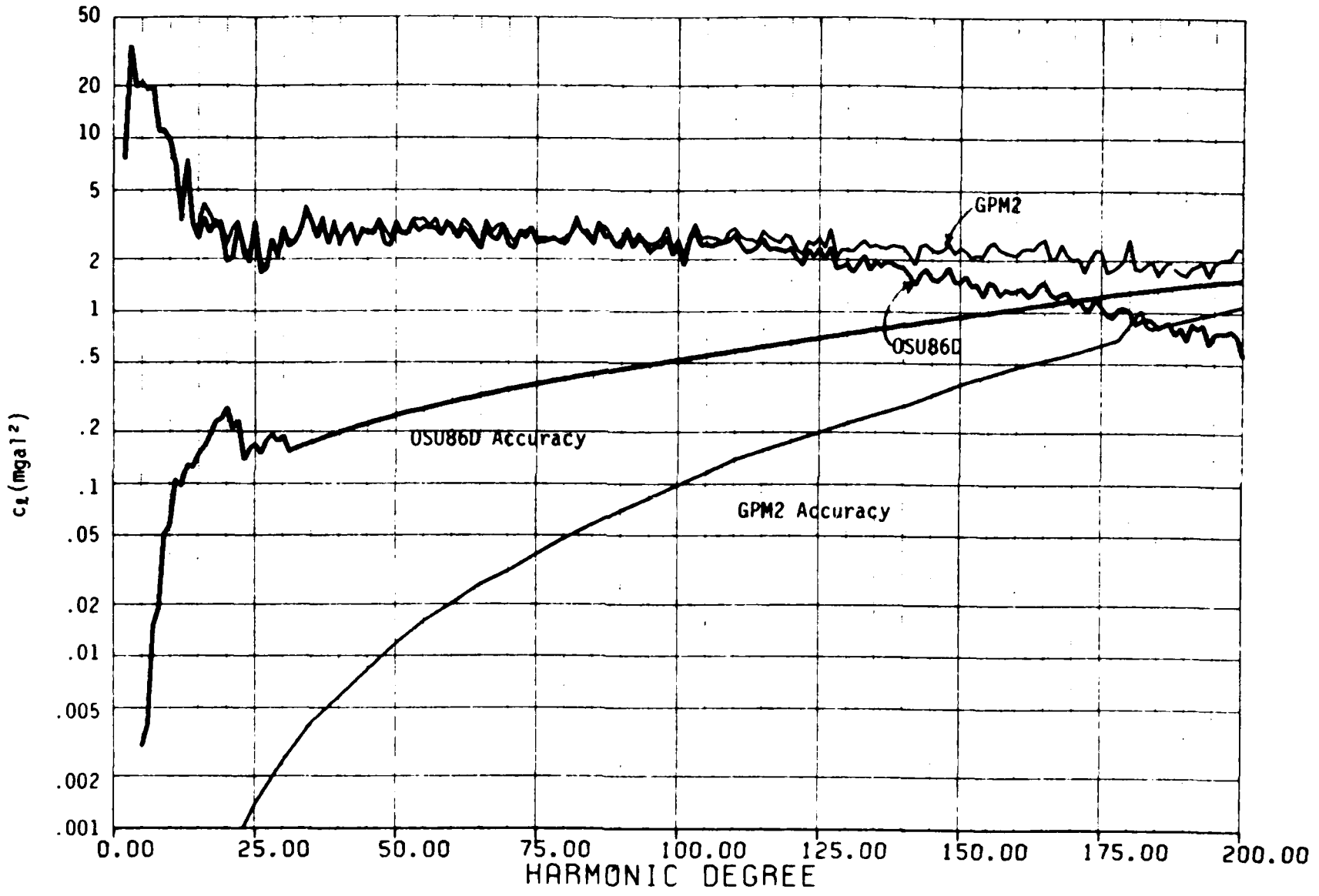

Figure 15. Anomaly Degree Variances and Their Accuracies for the OSU86D and the GPM2 Solution

8.4 Undulation Residual Correlation with Elevation

Tscherning (1985, private communication) pointed out that the differences in the Doppler and gravity model undulations were correlated with elevation for the OSU81 solution but not for the GPM2 field. In our research we have computed this correlation for several models for various Doppler data sets by assuming there was a linear correlation with elevation. Results for the global data set and the stations in Europe are shown in Table 23 and 24.

Table 23. Undulation Residual Correlation Using the Global Station Set

Solution	Slope (m/km)	Std Dev. (m/km)	No. of Stations
OSU81	0.73	± 0.16	1721
GPM2	0.00	0.10	1735
OSU86C	0.41	0.12	1741
OSU86D	0.43	0.12	1743

Table 24. Undulation Residual Correlation Using the European Station Set

Solution	Slope (m/km)	Std Dev. (m/km)	No. of Stations
OSU81	1.53	± 0.81	172
GPM2	1.87	0.63	172
OSU86C	0.92	0.65	172
OSU86D	1.14	0.69	172

From these results we see that the GPM2 model yields residuals with no elevation correlation for the global data set but significant correlation for the European stations. Tests described in Section 6.5 indicate that the correlation in the non-GPM2 solution arises from the gravity field information in degrees 7 thru 14. Further tests are needed to better understand the apparent correlation and its significance.

8.5 Correlation with Topography

Under certain assumptions the topography and its isostatic compensation can be considered to generate a portion of the earth's gravity field. It is appropriate to consider the correlation of the spherical harmonic representation of the topographic/isostatic potential and of the gravitational potential represented by various models. Such correlation, by degree, can be computed from equation (6.7). The average correlation for several different

Table 26. Root Mean Square Residual From Satellite Orbit Fits Using Selected Geopotential Models

	Potential Model			
Satellite	Standard*	86C	86D	GPM2
Starlette	± 47 cm	143	179	737 cm
Seasat	± 0.67 cm/s	1.39	1.46	1.76 cm/s
Oscar	± 1.52 cm/s	1.42	1.42	1.62 cm/s
BEC	± 75 cm	69	175	133 cm
Lageos	± 8 cm	8	8	16 cm
Lageos	± 7 cm	7	7	17 cm
Geos-2	± 134 cm	85	97	347 cm

* see text

The standard field used in Table 26 is a specific field that in some cases is a tailored geopotential model. Specifically the standard models are PGS1331 for Starlette; PGSS4 for Seasat; GEM10B for Oscar, BEC, and Geos-2; GEML2 for Lageos. The 86C/D and GPM2 models were used in the fits complete to degree and order 36.

9. Summary and Conclusions

It has been five years since our previous high degree expansion and combination solution had been carried out. Since then we have seen a number of developments that warranted the new solutions described in this report. These developments are in the data area; the theoretical area; and the computer area.

In the data area we have recently completed a new set of 1°x1° mean terrestrial gravity anomalies. This collection of anomalies has increased from our prior set and has improved estimates in a number of areas. In addition a set of ocean wide 1°x1° anomalies has been derived from the Geos-3/Seasat altimeter data. The merged terrestrial/altimeter data set provides a more complete and more reliable data had than used before. And finally, we had the GEML2 potential coefficient set and its revised accuracy estimates to use for our a priori solution.

In the theoretical area, several improvements have been made in the new solution. First, the boundary condition relating gravity anomalies and the disturbing potential was more precisely formulated to avoid a spherical approximation. Second, correction terms were formulated that enabled the integration over the surface of the ellipsoid as opposed to an integration over a spherical surface.

3. What is the smoothing effect on the potential spectrum from the use of the optimal estimation (or least squares collocation procedure)?

4. What is the best way to carry out a high degree expansion using 30'x30' mean values and what differences will be found with the 1° solution carried out for this study?

5. Sould Doppler derived geoid undulations be incorporated into the geopotential solution and if so, what parameters should be modeled?

6. What is the best way to balance the needs for a gravity near the earth's surface and in space?

7. Should geophysical anomalies be used at all in the solutions or should their use be restricted to locations where some independent verification is possible?

8. What is the reason for the residual undulation correlation with elevation found in most geopotential solutions?

9. What is the effect of using the full error variance-covariance matrix of the a priori potential coefficients.

10. What are the divergence problems for the potential series, and series representation of other gravimetric quantities, implied by these high degree spherical harmonic expansions?

Finally we should note that there is a strong need for an improved satellite potential coefficient set. Although GEML2 is strong at degrees below 6, substantial improvement is needed in the higher degrees. As such fields become available it will become reasonable to repeat the combination process to obtain an accurate representation of the earth's gravitational potential.

REFERENCES

Boucher, C. and Z. Altamimi, Towards an Improved Realization of the BIH Terrestrial Frame, in Proc. of the Int. Conf. on Earth Rotation and Terrestrial Reference Frame, Dept. of Geodetic Science and Surveying, The Ohio State University, Columbus, Vol. 2, 1985.

Colombo, O.L., Numerical Methods for Harmonic Analysis on the Sphere, Report No. 310, Dept. of Geodetic Science, The Ohio State University, Columbus, 1981.

Cook, A.H., The External Gravity Field of a Rotating Spheroid to the Order of e^3, Geophysical Journal, Vol. 2, No. 3, 199-214, 1959.

Pellinen, L.P., Effects of the Earth Ellipticity on Solving Geodetic Boundary Value Problem, Bolletino di Geodesia e Scienze Affini, Vol. 41, No. 1, pp. 89-103, 1982.

Papoulos, G., Implementation of Programs Used by Hajela for the Optimal Estimation of High Degree Spherical Harmonic Expansions, unpublished report, Dept. of Geodetic Science and Surveying, The Ohio State University, Columbus, December 1985.

Rapp, R.H., Analytical and Numerical Differences Between Two Methods for the Combination of Gravimetric and Satellite Data, Bolletino di Geofisica Teorica ed Applicata, Vo. XI, No. 41-42, pp. 108-118, 1969.

Rapp, R.H., A Global 1°x1° Anomaly Field Combining Satellite, GEOS-3 Altimeter, and Terrestrial Data, Dept. of Geodetic Science, Report No. 278, The Ohio State University, Columbus, 1978; AFGL-TR-78-0282,AD-A064 740

Rapp, R.H., Potential Coefficient and Anomaly Degree Variance Modeling Revisited, Report No. 293, Dept. of Geodetic Science, 22p, 1979; AFGL-TR-82-0019, AD-A113 098

Rapp, R.H., The Earth's Gravity Field to Degree and Order 180 Using SEASAT Altimeter Data, Terrestrial Gravity Data, and Other Data, Report No. 322, Dept. of Geodetic Science and Surveying, The Ohio State University, Columbus, Dec 1981.

Rapp, R.H., Geoid Undulation Computations for Doppler Positioning Requirements, in Proc. of the 43rd Annual Meeting, American Congress on Surveying and Mapping, Washington DC, 1983.

Rapp, R.H., The Determination of High Degree Potential Coefficient Expansions from the Combination of Satellite and Terrestrial Gravity Information, Report No. 361, Dept. of Geodetic Science and Surveying, The Ohio State University, Columbus, 1984.

Rapp, R.H., Gravity Anomalies and Sea Surface Heights Derived from a Combined Geos3/Seasat Altimeter Data Set, J. Geophys. Res., 91, B5, 4867-4876, 1986a.

Rapp, R., Global Geopotential Solutions, prepared for the Int. Summer School in the Mountains, Admont Austria, August 1986b.

Rapp, R.H. and J.Y. Cruz, Development and Comparison of High Degree Spherical Harmonic Models of the Earth's Gravity Field, paper presented at the Symposium, "Definition of the Geoid", Florence, Italy, May 1986.

Reigber, C., G. Balmino, H. Müller, W. Bosch, and B. Moynat, GRIM Gravity Model Improvement Using LAGEOS (GRIM3-L1), J. Geophys. Res., Vol. 90, B11, Sept. 1985.

END

3-87

DTIC